FUZZY COLOUR C-MEANS CLUSTERING FOR PATTERN SEGMENTATION IN HISTOLOGICAL IMAGES

G. Bueno*, R. González*, J. González**, M. García-Rojo**
* Universidad de Castilla-La Mancha, E.T.S.I. Industriales, Ciudad Real, Spain
** Hospital de Alarcos, Complejo Hospitalario de Ciudad Real, Spain
gloria.bueno@uclm.es

Abstract: This paper presents a colour fuzzy c-means algorithm to facilitate the segmentation of relevant structures in histological images. The fuzzy reasoning exploits *a priori* statistical information from several knowledge sources based on histogram analysis both of the colour and intensity. Thereby, the algorithm is applied iteratively at different colour spaces such a RGB (Red, Green and Blue), HSI (Hue Saturation and Intensity) and HSV (Hue Saturation and Value) to segment relevant structures: nucleus, nucleolus and glands. The method has been developed to assist pathologist in image evaluation and diagnosis of histological slides from prostate and bladder tissues.

Introduction

The first aim in automatic processing histological tissues is their segmentation into relevant structures, such as nucleus, nucleolus, glands, cytoplasm, etc.. These structures are mostly arranged into disordered patterns which make difficult its segmentation, [1-3]. Moreover, the intensity and colour variability of the images due to illumination conditions and the slide processing, make the segmentation of histological structures a difficult task and therefore still a challenge problem [4].

In the last few years many researches have been carried on to develop algorithms and image processing tools for histological image analysis. To this end, algorithms capable to enhance the nucleus and cytoplasm in histological images of the prostate have been done. These segmentation algorithms are based on statistical information at the HSI colour space [3]. Statistical theory combined with the Gleason grading system to provide accurate diagnosis. [4], and morphological theory [5], have been also exploited for classification purpose of cancerous tissues. Colour (RGB model) and morphometric properties joined by fuzzy logic. The method is applied to glandule, stoma and nuclei. A shape pattern for these structures has been previously set manually by expert pathologist. [6] and active contour models, [7, 8] have been also used to segment nucleus of histological images. These methods show limited results because they are mainly focused on a single structure or a type of tissue previously defined.

This paper presents a segmentation method based on fuzzy logic theory. It has been implemented to assist pathologist in image evaluation and diagnosis. Thus, the algorithm is able to identify relevant structures and properties of histological images. It uses statistical information provided by the HSI/HSV (Hue, Saturation and Intensity/Value), and the RGB colour histograms. The study of the image at different colour spaces allows us to choose the most suitable coordinates for analysing the structure under consideration. The algorithm has been applied to a data set composed of more than 100 images from the prostate and bladder. The proposed algorithm gives the capability of iteratively applied the FCM at different colour spaces. This provides a complete segmentation of all structures included in the image independently of their colour properties.

Next section describes the implemented method, taking into account the colour models analysis and the fuzzy logic theory. Then, the materials used and the results obtained are explained. Finally, the conclusions of this study are presented.

Methods

Colour models

Colour models are mathematical representations of a set of colours. Here we explain the most popular ones used in this study, that are the RGB, HSI and HSV.

RGB colour model

The RGB colour model is well known because it is the model used by the visualization systems. This model is based on a Cartesian coordinate system under a cube subspace. In this cube the RGB values are at three corners; and the CMY (cyan, magenta, yellow) are at the other ones, with the black colour at the origin. However, this colour space is not the most appropriate in digital image processing due to the intuitive notions of tonality (H), saturation (S) and intensity (I) are lost. An example of this situation appears when we work with the image intensity. If we use the RGB colour model, we will work with the three channels of the model, however if we use other colour models such as HSI or HSV, we will only work with the intensity channel (I or V) of these colour models [9-11]. To overcome this problem, in this study we have also considered the HSI and HSV models.

ISSN: 1727-1983

HSI colour model

The HSI colour model is widely used in digital image processing, since it separates the colour components H and S from the intensity (I) one. Moreover, the HSI colour model is closely related to the way human beings perceive colour. In this model H describes a pure colour, such as, yellow, red, orange, etc. and S measures the degree a pure colour is diluted with white light. The HSI colour model is represented by a double prism subspace based on the Maxwell triangle generated by the RGB cube subspace. This model is appropriated to develop algorithms working with the image intensity, since the channel is calculated as an average of the RGB colour model.

The conversion equations between the RGB and HSI colour models are as follows [3, 9].

The equations to transform an image from the RGB colour model into the HSI one, using normalized values within [0..1] are:

$$I = (R + G + B)/3 \tag{1}$$

$$S = 1 - (3 * \min(R, G, B)/(R + G + B)) \tag{2}$$

$$H = \cos^{-1}((0.5*((R-G)+(R-B)))/\sqrt{(R-G)^2+(R-B)*(G-B)}) \tag{3}$$

taking into account that:

- if B>G then H = 2* π - H
- if R = G = B then H = undefined and S = 0

Using these equations the ranges for each colour channel are:

- H $\in$ [0..2 π].
- S $\in$ [0..1].
- I $\in$ [0..1].

The equations to transform an image from the HSI colour model into the RGB one are:
if H = -1 then:

$$R = G = B = I \tag{4}$$

where I is given by equation (1)

if H < 2* π /3 then:

$$B = (1 - S)/3 \tag{5}$$

$$R = (1 + (S * \cos(H))/\cos(\pi/3 - H))/3 \tag{6}$$

$$G = 1 - (B + R) \tag{7}$$

if H < 4* π /3 then H = H - 2* π / 3 and:

$$R = (1 - S)/3 \tag{8}$$

$$G = (1 + (S * \cos(H))/\cos(\pi/3 - H))/3 \tag{9}$$

$$B = 1 - (G + R) \tag{10}$$

If H < 2* π then H = H - 4* π / 3 and:

$$G = (1 - S)/3 \tag{11}$$

$$B = (1 + (S * \cos(H))/\cos(\pi/3 - H))/3 \tag{12}$$

$$R = 1 - (G + B) \tag{13}$$

The obtained R, G and B values have been normalized by:

$channel_i = channel_j/(r + g + b)$

where: $channel_i$ is R, G or B, $channel_j$ is r, g or b. Thus, to get the correct values for each pixel in the RGB colour model the r, g, b components have been re-written as follows: r = 3*I*R, g=3*I*G and b=3*I*B.

HSV colour model

HSV colour model was proposed by A. Ray Smith in 1978 and it is based on the HSI and HSL model, where L is the lightness, [10, 11]. The HSV model may be represented by both a conical or cylindrical subspace. Where the tonality (H) is represented by a circular (HSI) or hexagonal (HSL) region; and a separated triangular or cylindrical region is used to represent the saturation (S) and the brightness value (V). The vertical axis represents the saturation and the horizontal axis represents the brightness. The cylindrical representation is mathematically the most appropriate and gives a wide range of saturation levels. Nevertheless the different saturations levels that the human visual system may perceive is lower when we are near the black (cone vertex), where it becomes closer to the conical model, [10].

The equations to transform an image from the RGB colour model to the HSV one, are [11]:

if R = MAX then:

$$H = \left(0 + \frac{G - B}{MAX - MIN}\right) * 60$$

if G = MAX then:

$$H = \left(2 + \frac{B - R}{MAX - MIN}\right) * 60 \tag{14}$$

if B = MAX then:

$$H = \left(4 + \frac{R - G}{MAX - MIN}\right) * 60$$

$$S = \frac{MAX - MIN}{MAX} \tag{15}$$

$$V = MAX \tag{16}$$

where MAX and MIN are the maximum and the minimum of the R, G, B values, respectively.

ISSN: 1727-1983

The HSV values are normalised such as, S and V belongs to [0..1] and H goes from 0 to 360 degrees..

Some constrains of this colour model are:

- If maximum = minimum (S = 0) then H is undefined. H is undefined because if S = 0 then we are moving though the grey line and therefore the tonality has no sense.
- If maximum = 0 (V = 0) then S is undefined. If V = 0 then we are representing a pure black, thus saturation and tonality have no sense

for these cases, typical of the cylindrical subspace the conical subspace is considered, then S is calculated by:

$$S = MAX - MIN \tag{17}$$

The equations to transform an image from the HSV colour model to the RGB colour model are:

if S = 0 then:

$$R = G = B = V \tag{18}$$

else

$$H_I = \left\lfloor \frac{H}{60} \right\rfloor \quad \text{and} \quad f = \frac{H}{60} - H_i$$
$$p = V * (1 - S)$$
$$q = V * (1 - (S * f))$$
$$t = V * (1 - (S * (1 - f))) \tag{19}$$

if H_i=*0* then $R = V, G = t, B = p$
if H_i= *1* then $R = q, G = V, B = p$
if H_i= *2* then $R = p, G = V, B = t$
if H_i= *3* then $R = p, G = q, B = V$
if H_i= *4* then $R = t, G = p, B = V$
if H_i= *5* then $R = V, G = p, B = q$

In order to use the HSI and HSV colour models, the following steps have been applied:

1. Change coordinates from the RGB colour model to the colour model we want to work with.
2. Apply the image processing algorithm (fuzzy C-means clustering) to the image.
3. Transform the image from the HSI or HSV colour model to the RGB one in order to display and store it.

Next section explains the fuzzy logic theory and the segmentation algorithm developed using this theory under the previously presented colour models.

Fuzzy C-Means Clustering (FCM)

The fuzzy logic theory tries to facilitate the segmentation of relevant structures in histological images. The FCM algorithm groups the pixels of an image studying their membership to a number of classes or clusters previously defined. The fuzzy membership function constrained to be between 0 and 1, reflects the degree of similarity between the data value at that location and the centroid of its class. Thus, a high membership value near 1 means that the pixel is close to the centroid for that particular class. The classes are defined by a centroid. The value of each centroid is going to be used to study the membership of a pixel to a class. In this case we are working with colour images and for this reason each centroid and pixel of an image are composed of three values that correspond to the three channels of the different colour models (RGB, HSI or HSV). We use x_1, x_2 and x_3 to define the values of the three channels of each pixel of an image and v_1, v_2 and v_3 to define the values of the three channels of each class or centroid.

Then, the FCM algorithm finds the optimal centroid for each class. The FCM algorithm is then formulated as the minimization of the squared error with respect to the membership functions, U, and the set of centroids V:

$$J(U,V:X) = \sum_{i=1}^{c}\sum_{k=1}^{n}(u_{ik})^m \left\| x_{jk} - v_{ji} \right\| \forall j = 1,..,3 \tag{17}$$

where u_{ik} is the membership of the pixel x_{jk} in class i and m >= 1 is a weighting exponent of each fuzzy membership, j is the channel number.

In this equation u_{ik} is defined as:

$$u_{ik} = \left[\sum_{n=1}^{c} \left(\frac{\left\| x_{jk} - v_{ji} \right\|}{\left\| x_{jk} - v_{jn} \right\|} \right)^{\frac{2}{m-1}} \right]^{-1} \quad \forall i,k,j = 1...3 \tag{18}$$

and each centroid $\vec{v}_i$ belonging to V is defined as:

$$\vec{v}_i = \frac{\sum_{k=1}^{n} (u_{ik})^m \vec{x}_k}{\sum_{k=1}^{n} (u_{ik})^m} \quad \forall i,k \tag{19}$$

where $\vec{v}_i = (v_{1i}, v_{2i}, v_{3i})$ so:

$$\forall v_{ji}, \quad v_{ji} = \frac{\sum_{k=1}^{n} (u_{ik})^m x_{jk}}{\sum_{k=1}^{n} (u_{ik})^m} \qquad j = 1,..3 \tag{20}$$

That is a study based on the distances of each pixel intensity to the centroids of each class. Iterating through these conditions leads to a grouped coordinate descent scheme for minimizing the objective function.

ISSN: 1727-1983

The stop criterion is determined for each iteration by $E_i < \varepsilon$ where:

$$E_i = \sum_{i=1}^{c} \left\| v_{ji,t+1} - v_{ji,t} \right\| \quad \forall t, j = 1,..,3 \qquad (21)$$

Once the method has converged a matrix with the membership or degree to which every pixel is similar to all of the *c* classes is obtained. Finally, the maximum membership, $\max(u_{ik})$, is assigned for x_{jk} FCM segmentation.

The values of the image pixels and the centroids depend on the colour model used and the channels where the fuzzy C-means is applied. Thus, the set of centroids is calculated based on the histogram analysis, and corresponds to the number of relevant structures contained in the image. The ranges for the different channels of the colour models used in this study are:

- The three RGB channels and the intensity component (I or V) of the HSI and HSV colour models takes values that go from 0 to 255.
- The tonality component (H) of the HSI and HSV models takes values from 0 to 360 degrees.
- The saturation (S) of the HSI and HSV colour models takes values that go from 0 to 100.

The decision of working with a specific colour model and with one or several channels for the segmentation algorithm depends on the statistical information obtained previously from the colour histograms (RGB, HSI and HSV). That is, the FCM algorithm is applied iteratively onto the most prevalent coordinates in order to segment the histological structures out. Each image at each iteration represents a set of relevant structures, that is a set with a single or several structures, where the original colour and intensity properties are recovered. Then, a statistical analysis is carried on again to set the fuzzy coordinate and the colour model and the segmentation algorithm is applied iteratively onto the images to get structures that are contained into others. This methodology allows pathologists to get structures that are very difficult to distinguish and segment using the segmentation algorithm directly.

The image data used in this study is described in the next section.

Materials

The segmentation algorithms developed have been applied to histological images at different resolutions and qualities. The data set used is composed of more than 100 microscopic images from the bladder and prostate area, containing different grades of malignancy.

The images from the prostate have been provided by the Hospital de Alarcos at Ciudad Real and images from bladder were provided by the IMIM (Medical Research Institute) at Barcelona.

The histological images of the prostate have been obtained using a digital camera of 3,34 Mpixels together with an optical microscopy. These images have been taken at different resolutions of 4x, 10x, 20x and 40x.

Image acquisition using digital cameras and optical microscopes allows pathologists to get high resolution images, but the quality of these images is lower than the images that can be obtain using the new equipments that allow pathologists to digitalize tissues directly. The illumination problem is solved using the new equipments.

The use of digital cameras and optical microscopes present problems concerning to the quality of the histological images [12, 13]. These problems are:

- Problems of illumination, colour and dynamic ranges.
- Loss of quality due to the image format (JPEG) and problems when the CCD has to represent blues tonalities.
- Problems to represent the differences of tonality when the CCD is situated in the dark parts of an image.

In the other hand the pathological images of the bladder have been taken using new equipment that can digitalize the images directly and the pathologist can display them. These images have different zooms (5x, 10x y 40x) and have been taken in the IMIM (Barcelona). The equipment has been developed by Leica Microsystems and allows pathologist to digitalize images using different resolutions, qualities and image formats.

These images and some results applying iteratively the FCM algorithm are shown in the Results section.

Results

Some segmentation results are presented. The size and zoom of the original images, the fuzzy components, the colour model and the number of centroids used are indicated on the figure captions. The error, ε, used in all these processed images is equal to 0.5.

The computational time processing the images on a PC (3GHz and 1GB RAM) under Windows XP has been calculated for 2 different compiler. The average computational time for the:

- minimum image size (720 x 540) with the windows compiler is 6.38s with the ICC compiler is 2.1s
- maximum image size (3900 x 3090) with the windows compiler is 25.2min with the ICC compiler is 8.2min

This shows that the use of a specific compiler and the optimizations supported by them make the segmentation algorithm more efficient.

ISSN: 1727-1983

In figure 1.b) the contours of the several segmented structures are displayed together with the original image, just for visualization purpose.

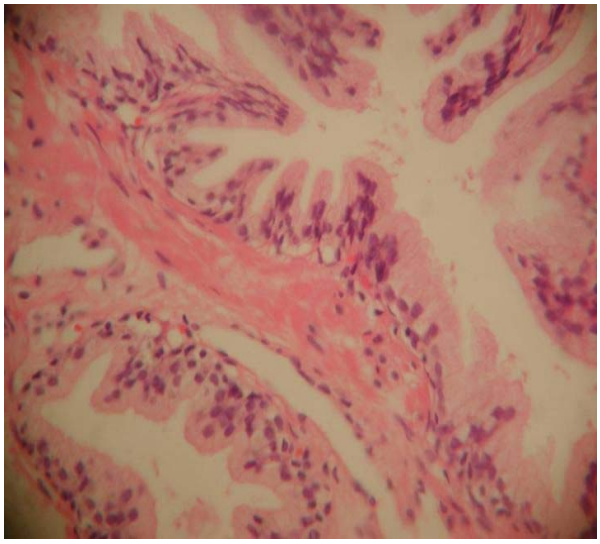

a) Original Image (prostate) 720 x 540 - 20x.

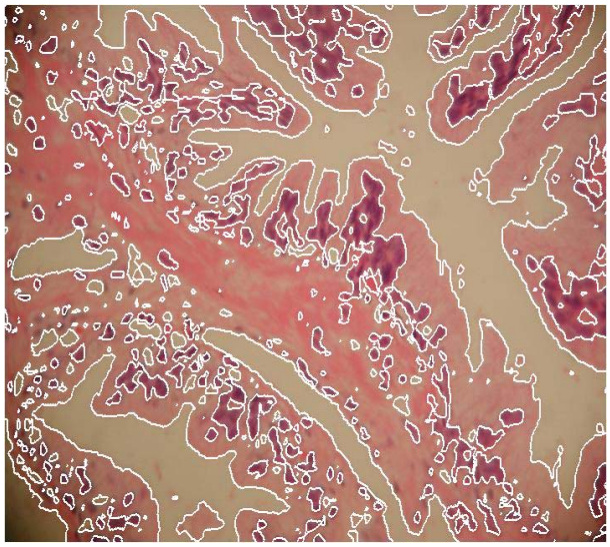

b) FCM Segmentation on H (HSI, 3 centroids).

Figure 1: FCM Segmentation under HSI colour model

Figure 2.c), 3.c) and 4.c) show how the nucleolus are obtained just after two iterations of the FCM algorithm, applied to the 3 RGB channels and with different number of centroids at each iteration.

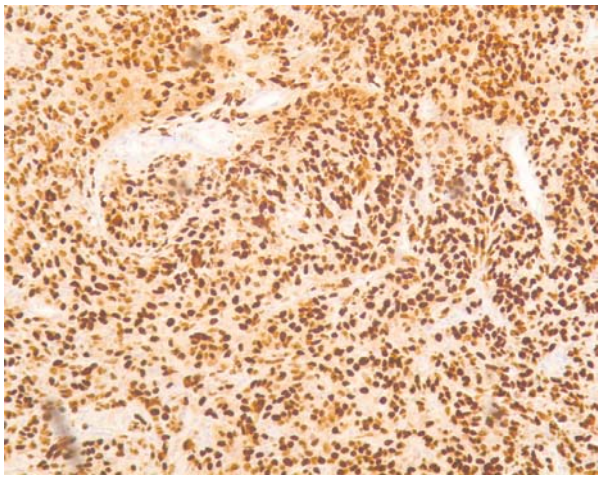

a) Original Image (bladder) 3900 x 3090 - 10x.

b) FCM Segmentation 1st iteration (RGB, 2 centroids).

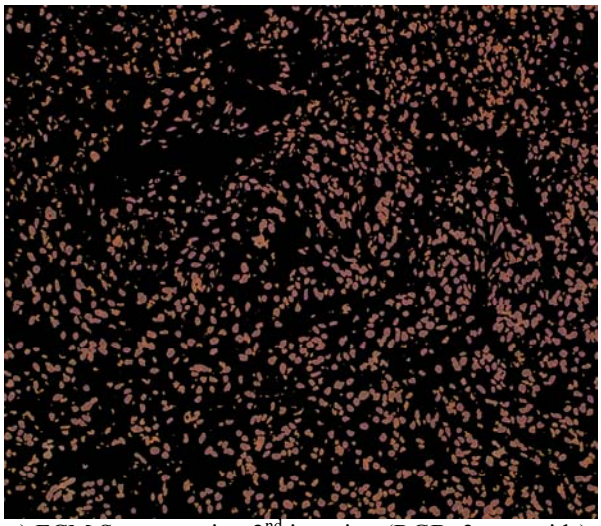

c) FCM Segmentation 2nd iteration (RGB, 3 centroids).

Figure 2: FCM Segmentation under RGB colour model

ISSN: 1727-1983

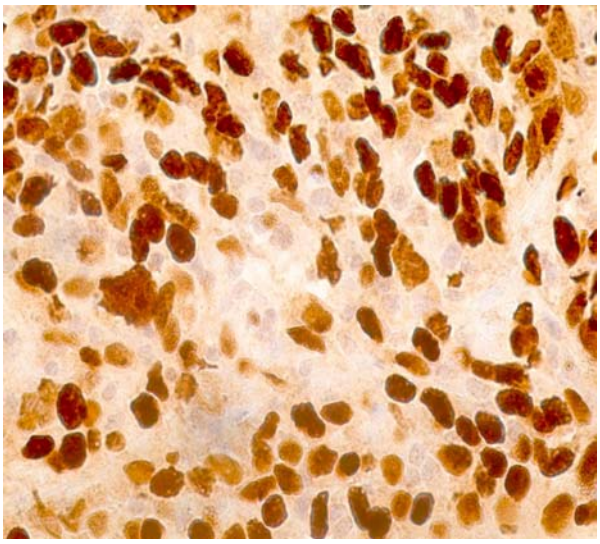

a) Original Image (bladder) 1300 x 1030 - 40x.

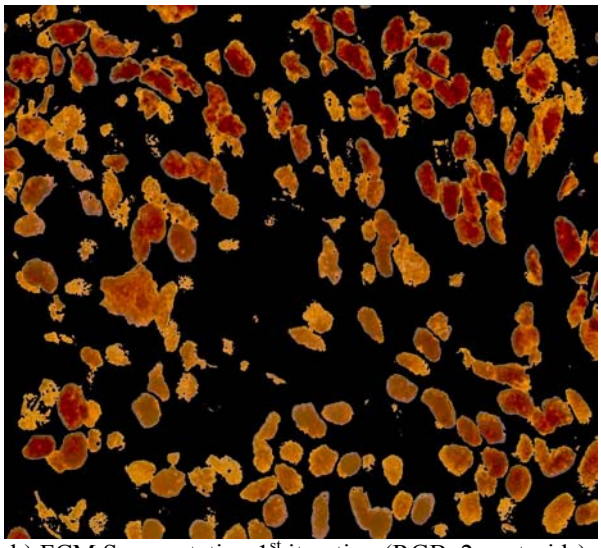

b) FCM Segmentation 1st iteration (RGB, 2 centroids).

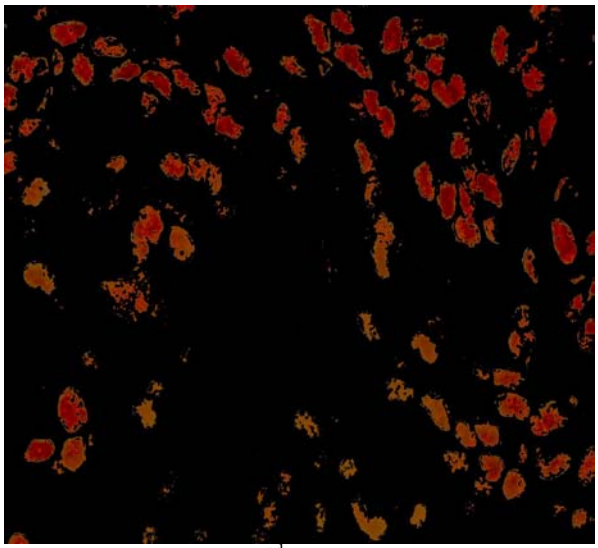

c) FCM Segmentation 2nd iteration (RGB, 4 centroids).

Figure 3: FCM Segmentation RGB model

.

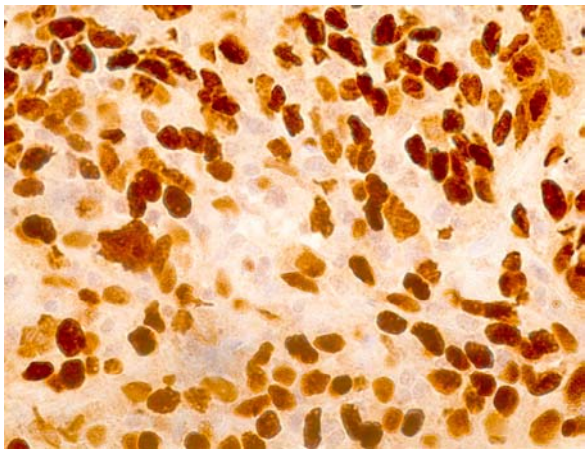

a) Original Image (bladder) 2600 x 2060 - 40x

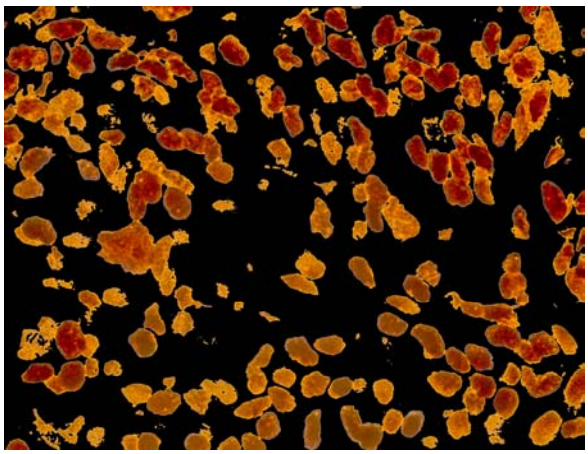

b) Segmented structures (RGB, 2 centroids).

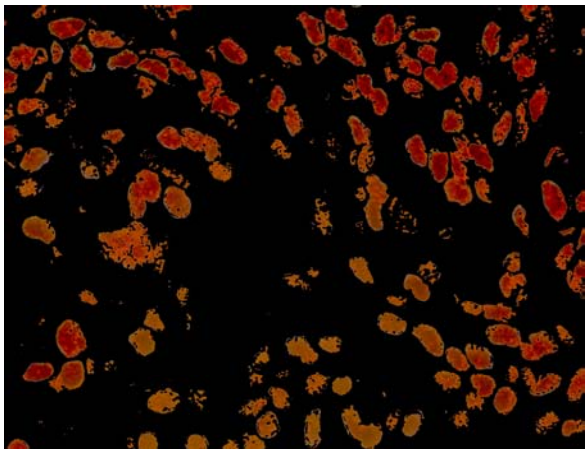

c) Segmentation of nucleolus (RGB, 3 centroids).

Figure 4: FCM Segmentation RGB model

Figure 5.c) show similar results than the previous ones for the nucleolus contained on image 6.a) but combining 2 colour models RGB for the 1st iteration and HSI for the 2nd one. The FCM algorithm for both iterations has been carried on at the 3 channels.

ISSN: 1727-1983

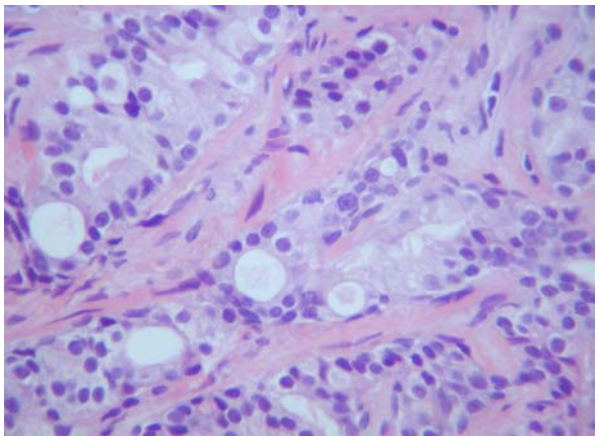

a) Original Image (prostate) , 2048 x 1536 - 40x

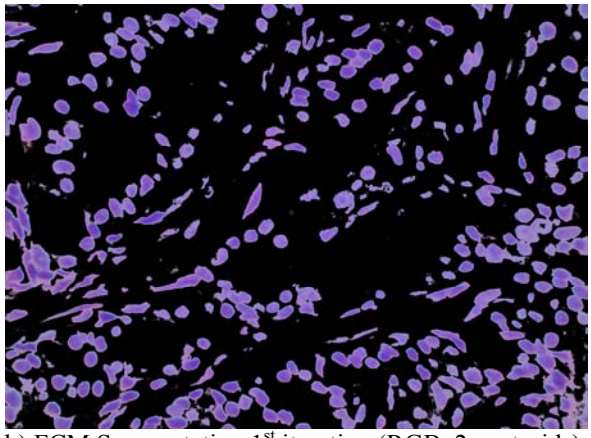

b) FCM Segmentation 1st iteration (RGB, 2 centroids).

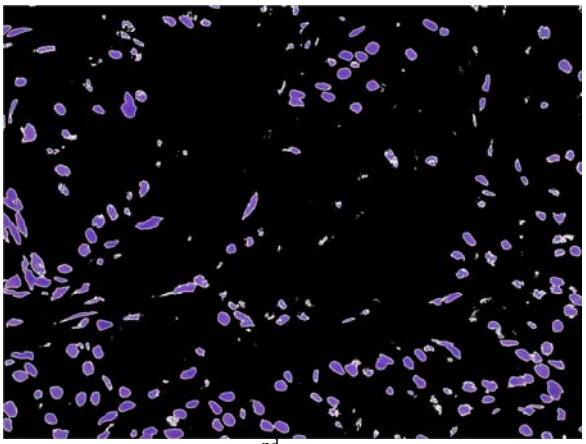

c) FCM Segmentation 2nd iteration (HSI, 4 centroids).

Figure 5: FCM Segmentation RGB and HIS model

Figure 6.b) shows the segmentation of the glands on a prostate sample image after one iteration of the FCM algorithms applied to the 3 HSI channels with 2 centroids.

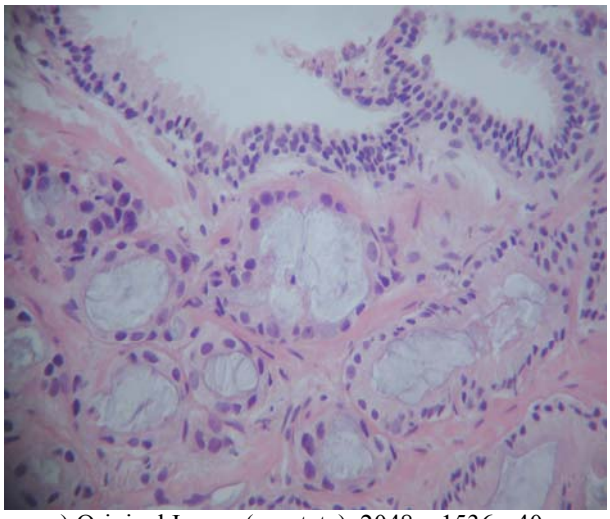

a) Original Image (prostate), 2048 x 1536 - 40x

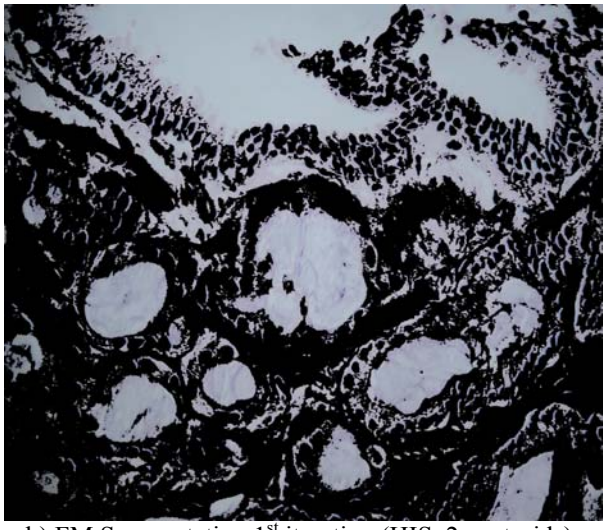

b) FM Segmentation 1st iteration (HIS, 2 centroids).

Figure 6: FCM Segmentation HIS model

The results have been qualitatively validated by pathologist experts. This validation shows that the implemented algorithm is a potential tool to segment relevant structures on histological images. Nevertheless further algorithms must be developed to obtain the overall objective of classifing the segmented structures from the sample tissues. Some future developments undergo are the adition of morphological properties to the colour one into the fuzzy clustering and reduce the processing time. The workload of these algorithms is very high, thus the requirements of memory and time must be improved. Therefore, the decision of using a specific compiler, such as, Windows Compiler or INTEL is very important. Moreover, further work will be done to parallel these algorithms in order to process bigger images.

ISSN: 1727-1983

Conclusions

The use of fuzzy colour clustering has proved to be a successful processing tool for segmentation. Therefore, the FCM algorithm described in this paper, based on the previous analysis of the histogram at different colour models has shown to be a powerful tool for the segmentation of relevant histological structures.

The capability of the algorithm to carry the fuzzy clustering on the most prevalent colour component (H, S, I – RGB, V) and on a different number of channels is a valuable property to facilitate and obtain the final segmentation. Moreover, to obtain segmentation of all structures it will be useful information for future classification purpose.

Further work is undergoing to reduce the processing time and to improve the segmentation, aiming to a successful classification of the histological structures and the sample tissue.

Acknowledgement

This research has been funded thanks to the projects INBIOMED ISCIII-G03/160 and MEC/PBI-03-017.

References

[1] BAMFORD, P.; LOVELL, B. (2001): **'**Method for accurate unsupervised cell nucleus segmentation', Proc. 23rd Internat. Conference of the IEEE Engineering in Medicine and Biology Society, 2001, Vol. 3, p. 2704 – 2708

[2] TANAKA, T.; JOKE, T.; OKA, T. (2001): 'Cell nucleus segmentation of skin tumour using image processing'**,**. Proc. of the 23rd Annual International Conference of the IEEE Engineering in Medicine and Biology Society, 2001, Vol. 3, p. 2716 - 2719

[3] GAO M., BRIDGMAN P. and KUMAR S. (2003): 'Computer Aided Prostate Cancer Diagnosis Using Image Enhancement and JPEG2000', Proc. SPIE International Conf. on Applications of Digital Image Processing, 2003, Vol. 5203, p. 323-334

[4] TEVEROVSKIY M., KUMAR V., MA J., KOTSIANTI A., VERBEL D., TABESH A., PANG H., VENGRENY Y., FOGARASI S. and SAIDI O.(2004): 'Improved Prediction of Prostate Cancer Recurrence Based on an Automated Tissue Image Analysis System'. Proc. IEEE Int. Symp. Biomed. Imaging, Arlington, VA, Apr. 2004, p. 257-260

[5] THIRAN J.-P. and MACQ, B. (2004): **'**Morphological feature extraction for the classification of digital images of cancerous tissues'**,** IEEE Transactions on Biomedical Engineering, Vol. **43**(10), p.:1011 - 1020 .

[6] BEGELRNAN, G., GUR, E., RIVLIN, E., RUDZSKY, M. and ZALEVSKY, Z. (2004): 'Cell Nuclei Segmentation Using Fuzzy Logic Engine' Proc. of .IEEE Intern. Conference on Image Processing, ICIP'04, p. 2937- 2940

[7] HU M.; PING X. and DING Y. **(**2004): 'Automated cell nucleus segmentation using improved snake**'**, Proc. Intern. Conference on Image Processing, ICIP '04. Vol. 4, p. 2737 - 2740

[8] YANG L., MEER P. and FORAN D.J (2005): 'Unsupervised Segmentation Based on Robust Estimation and Colour Active Contour Models' IEEE Trans. on Information Technology in Biomedicine, **9**.

[9] GONZALEZ R.C.; WOODS R.E. (1993): 'Digital Image Processing' Addison-Wesley

[10] HEARN D. and BAKER M. (1997): 'Computer Graphics' Prentice-Hall

[11] FOLEY.; van Dam.; and FEINER, HUGHES. (1997):'Computer Graphics: Principles and Practice' Addison-Wesley

[12] RILEY RS. (2004): 'Digital photography: a primer for pathologists', J Clin Lab Anal **18**, p. 91-128

[13] LAMMINEN H. (2001): 'Medical applications and technical standardization of teleconference', Acta Electronica Universitatis Tamperensis 106.. Internet site address: http://acta.uta.fi/pdf/951-44-5096-5.pdf

[14] FERRERES L, GARCÍA ROJO M, PURAS GIL AM. (2001): 'Manual de Telepatología.- SEAP'. Internet site address: http://www.seap.es/telepatologia/

ISSN: 1727-1983